Effect of the Vacuum Pressure and the Working Fluid Inventory to the Maximum Heat Loading (Qmax) of the Heat Pipe

Wei-Keng Lin[1]; Chen-I Chao[2]; Tzou, Y.M. Calvin[2]; G. H. Hsu[3]; S.M.Chou[4]
[1]Professor, National Tsing-Hua University, ESS Dept., Sin-Chu City, Taiwan, 300
[2]Ph.D. Student, National Tsing-Hua University, ESS Dept., Sin-Chu City, Taiwan, 300
[3]M.S. Student, National Tsing-Hua University, ESS Dept., Sin-Chu City, Taiwan, 300
[4]Associate Professor, Chinese Culture University, Chem. & Matl. Dept., Taipei, Taiwan, 111
TEL:+886-3-5715131 Ext 42664 E-mail:wklin@ess.nthu.edu.tw

ABSTRACT

Over the last decade, the computer clock speed drastically increases as the chip manufacturing technique improves. Heat pipe generally is already applied to the heat-removed system, the notebook and other equipments. Due to the reason of the operation temperature of the CPU need to less than 100℃, a high vacuum status of the heat pipe must design for achieved to high heat transport ability. Therefore, the heat pipe performance ability not only depends on the geometric parameters such as heat pipe wall thickness、tube material etc., but also depends on the working fluid thermo properties such as latent heat, vapor pressure, viscosity, inventory and vacuum pressure etc.

The purpose of this study was to evaluate the effect of the inventory and the vacuum pressure to the maximum heat transport ability of the heat pipe. The experiment was operated under the vacuum pressure of the heat pipe at the range of 0.1torr to 10torr, while the inventory was controlled with the range of 0.5ml to 1ml. The results shown the errors between the experimental data and the theoretical value were within 10%. The experiment was also shown when the higher of the vacuum pressure, the lower of the non-condensable gas (NCG), the higher of the maximum heat transport ability (Q_{max}). The curve for the Q_{max} with respect to the vacuum pressure turns out to be an exponential function.

Keywords: *Heat Pipe, Vacuum Pressure, Maximum Heat Transfer, Non-condensation Gas (NCG), inventory*

1. INTRODUCTION

The first heat pipe was tested at Los Alamos National Laboratory in 1963 [1]. Since then, heat pipes have been used in various devices such as laptop computers, spacecraft, plastic injection molders, medical devices, and lighting systems. A typical heat pipe comprises a sealed pipe made of a material having a high thermal conductivity, such as copper. A vacuum pump is used to evacuate all fluids (both vapor and liquids) from a vacuum heat pipe, and then, the pipe is filled with a fraction of a percent by volume of a working fluid, (or coolant), chosen to match the operating temperature [2][3]. Due to partial vacuum that is near or below the vapor pressure of the fluid, some amount of the fluid is in the liquid phase, while some of it is in the vapor phase. Inside the pipe, an optional wick structure exerts a capillary pressure on the liquid phase of the working fluid. This is typically a sintered copper powder or a series of grooves parallel to the pipe axis; however, it may be any material that is capable of exerting capillary pressure on the condensed liquid to wick it back to the heated end.

When heat transfer begins, the inventory and vacuum pressure plays a very important role in the heat dissipation ability of the heat pipe. If a sealed heat pipe was charged too much of working fluid, there were no enough space in heat pipe for liquid to vaporized, and two-phase heat exchange could not occurred easily. On the contrary, if the inventory was too little, the heat pipe performance could not reach to the optimal state. If a sealed heat pipe has a high vacuum pressure, two-phase heat exchange can occurred easily. On the other hand, if the heat pipe has a low vacuum pressure, the NCG gas would block the vapor channel and result in very poor heat dissipation [4][5]. When made the heat pipe in the laboratory, the general first step was evacuated the gas from heat pipe, then fill with working fluid secondary. However, for the reason of mass production, heat pipe manufacturers first charged the working fluid into the whole bunch of the heat pipes in the same time, and then evacuate the gas simultaneously. Therefore, this procedure does not reveal the actual vacuum pressure, and people desire to know how to detect the real inventory and the actual vacuum pressure of heat pipe.

2. THEORETICAL MODEL

Consider the pressure drop due to the non-condensable gas ΔP_{NCG} was exist in the heat pipe, than the total capillary pressure drop ΔP_C had to be larger than sum of the component pressure drop as shown as in equation (1)

$$\Delta P_c \geq \Delta P_l + \Delta P_v + \Delta P_g + P_{NCG} \tag{1}$$

Define total friction factor due to viscosity and wick effect from liquid and vapor [6]:

$$M_f = \left[\frac{\mu_l}{\rho_l A_w K_w} + f' \left(\left(\frac{\mu_l}{\rho_l A_w L_c r_w}\right) + \left(\frac{\mu_v}{\rho_v A R_i L_e}\right) \right) \right] \tag{2}$$

the pressure drop ΔP_{cg}:

$$\Delta P_{cg} = \Delta P_c - \Delta P_g = \left(\frac{2\sigma_l}{r_w} - \rho_l g L_{eff,l} \sin\phi \right) \tag{3}$$

The maximum heat transport happened at operating temperature (adiabatic temperature) T_a:

$$Q_{\max\_T_a} = \frac{\left(\frac{2\sigma_l}{r_w} - \rho_l g L_{eff,l} \sin\phi \right) h_{fg\_T_a}}{\left[\frac{\mu_l}{\rho_l A_w K_w} + f' \left(\left(\frac{1}{L_c}\right) \frac{1}{A_w r_w} \left(\frac{\mu_l}{\rho_l}\right) + \left(\frac{1}{L_e}\right) \frac{1}{A_i R_i} \left(\frac{\mu_v}{\rho_v}\right) \right) \right] L_{eff}} \tag{4}$$

(A) Effect of the vacuum pressure to the performance of the heat pipe

Plug eq. (1), eq. (2) into eq. (4), rearrange:

$$Q_{\max\_T_a} = \frac{(\Delta P_{cg} - P_{NCG}) h_{fg\_T_a}}{M_f L_{eff}} \tag{5}$$

Let $Q_{max\_Ta,0}$ represented the maximum heat transport withou any NCG:

$$Q_{\max\_T_a,0} = \frac{\Delta P_{cg} h_{fg\_T_a}}{M_f L_{eff}} \tag{6}$$

Therefore, eq. (5) turn to be:

$$Q_{\max\_T_a} = Q_{\max\_T_a,0} - \frac{P_{NCG} h_{fg\_T_a}}{M_f L_{eff}} \tag{7}$$

Rearrange eq. (7) :

$$Q_{\max\_T_a} = Q_{\max\_T_a,0} \left(1 - \frac{P_{NCG} h_{fg\_T_a}}{Q_{\max\_T_a,0} M_f L_{eff}} \right) \tag{8}$$

Plug eq.(6) into eq.(8):

$$Q_{\max\_T_a} = Q_{\max\_T_a,0} \left(1 - \frac{P_{NCG}}{\Delta P_{cg}} \right) \tag{9}$$

Let $x = \left(\frac{\Delta P_{NCG}}{P_{Cg}}\right)$, and according to the Taylor Series:

$$e^{(-x)} = \sum_{n=0}^{n=\infty} \frac{x^n}{n!} = 1 + (-x) + \frac{(-x)^2}{2!} + \frac{(-x)^3}{3!} + ... \tag{10}$$
$$\cong 1 - x \quad (\text{if } x << 1)$$

$$1 - x = 1 - \left(\frac{P_{NCG}}{\Delta P_{Cg}}\right) = e^{-\left(\frac{P_{NCG}}{\Delta P_{Cg}}\right)} \tag{11}$$

The maximum heat transport with NCG:

$$Q_{\max\_T_a} = Q_{\max\_T_a,0} \times e^{-\left(\frac{P_{NCG}}{\Delta P_{Cg}}\right)} \tag{12}$$

Eq. (12) shown when the vacuum was more higher (fig. 1), the maximum heat transport was getting reach to $Q_{max\_Ta,0}$ ($Q_{max\_Ta} \fallingdotseq Q_{max\_Ta,0}$), when the NCG was getting more in the heat pipe, the maximum heat transport reached to a constant.

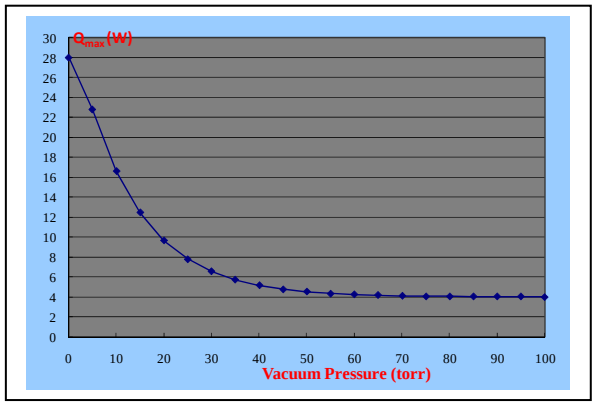

Fig.1. Vacuum pressure with respect to Q_{max_Ta}

(B) The calculation for the inventory

Assume V_{pore} was the space volume of the wick which could represented by the eq.(13):

$$V_{pore} = \pi (R_O^2 - R_i^2) \times L_{eff} \times \varepsilon \tag{13}$$

where ε was the porosity of the wick structure. V_{tot} was the total space volume of the heat pipe and represented by the eq. (14)

$$V_{tot} = \pi R_i^2 \times L_{eff} + V_{pore} \tag{14}$$

Since the minimum working fluid inventory was V_{pore}, however, the in realistic state, the inventory should a little bit larger than V_{pore} and less than the total space volume of the heat pipe. Therefore:

$$V_{tot} > \frac{m_l}{\rho_l} > V_{pore} \tag{15}$$

let β was the ratio of the space volume of the wick to the total space volume of the heat pipe:

$$\beta = \frac{V_{pore}}{V_{tot}} \tag{16}$$

V^+ was the ratio of the inventory to the product

of the V_{tot} and ρ_l :

$$V^+ = \frac{m_l}{V_{tot}\rho_l} \quad (17)$$

Therefore, the requirement for the working fluid inventory was generally following eq. (18), it was also implying that eq. (18) was a very simple indicator for whether the inventory was good enough or not.

$$1 > V^+ > \beta \quad (18)$$

3. EXPERIMENTAL FACILITY

The heat pipe performance curve was measured at a constant adiabatic temperature (for instance: 40℃). When the test was begining, the heat flux is low, the heat was transported to the liquid surface partly by conduction through the wick and the liquid and partly by natural convection [7]. Evaporation occurs from the liquid surface. As the heat flux increases, the liquid that is in contact with the wall becomes progressively superheated, and bubbles are formed at the nucleation sites. These bubbles transport energy from the sites to the liquid surface through the latent heat of vaporization and increase the convective heat transfer greatly. With a further increase in the heat flux, the critical value (burnout) at which the wick dries out and the heat pipe ceases to operate is attained. The heat pipe performance curve measurement flow chart was shown as in figure 2.

The schematic diagram of the test facility shown in figure 3 was include a DC power supply, thermostat, flowmeter, heat pipe test platform and a PLC used to keep adiabatic temperature constant. Fig. 4 showed a tipical case for the maximum heat loading of the heat pipe occurred at 54W.

4. RESULTS AND DISCUSSION

Table 1 shown all the geometry parameters for this study. By pluging in these parameters into equ. (4), one might obtain the theoretical value for the $Q_{max\_40C\_theory}$ at operating temperature 40℃. Table 2 shown the comparison of the theoretical values ($Q_{max\_40C\_theory}$) with the experiment data ($Q_{max\_40C\_exp}$) at different working fluid inventory and different vacuum pressure. The experiment results shown the relative error (Er.1) of the maximum heat loading of the theoretical values and experimental data was within 10% at different vacuum pressure.

$$Er.1(\%) = \frac{(Q_{max\_40C\_theory} - Q_{max\_40C\_exp})}{Q_{max\_40C\_exp}} \times 100\% \quad (19)$$

Figure 5 to figure 9 shown the maximum heat loading with respect to the vacuum pressure for the theoretical cuve and experimental curve from 0.7ml to 1.1ml. the Q_{max} was decreased with increasing of the vacuum pressure. From figure 5 to figure 9, one may notice that both the theoretical curve and experimental curve were quite match. The experiment results were also imply that the performance of these heat pipe was not good compare with the commercial heat pipe, the reason that the performance was not good could be due to all the heat pipe was not clean enough. plug P_{NCG}, ΔP_{cg} and experiment data Q_{max_Ta} into eq. (11), one might obtain $Q_{max\_Ta,0}$ with respect to different vacuum pressre. Theoretically, $Q_{max\_Ta,0}$ should be the same at the same inventory, therefore, the relative error (Er.2) could be calculated from eq. (20):

$$Er.2(\%) = \frac{(Q_{max\_40C,0} - Q_{max\_40C,avg})}{Q_{max\_40C,avg}} \times 100\% \quad (20)$$

Table.3 showed the comparison of the Q_{max_40C} at different inventory for P_{NCG} =0 and T_a=40℃. The error (Er.2) was within 10%. Fig. 10 was the effect of the inventory to the maximum heat loading of the heat pipe. Obviously, the optimization for the working fluid inventory was 0.8ml in this study. Table 4 showed the V^+ with respect to different inventory. When at inventory was 0.7ml, the V^+ condition was unsatisfied the eq. (18) and that explained that why Q_{max} was not good compare with that of the inventory at 0.8ml.

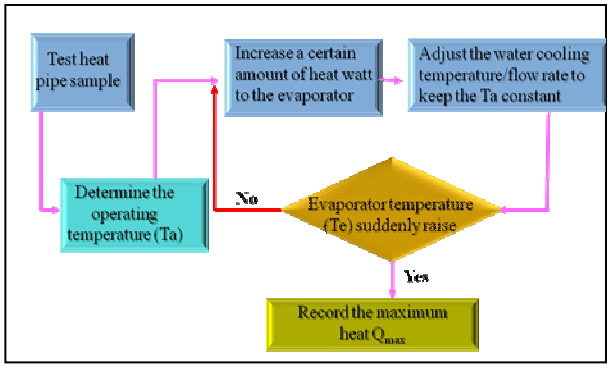

Fig.2 Flow chart for the heat pipe performance curve measurement

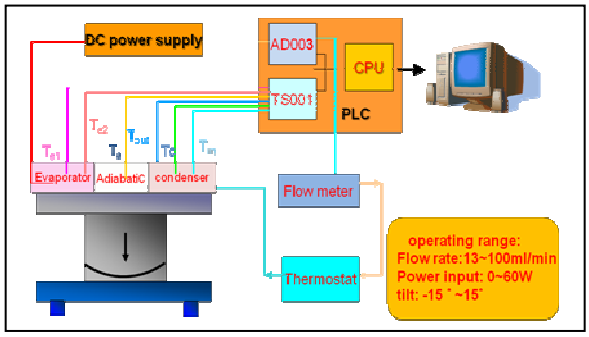

Fig.3 Schematic diagram of the test facility

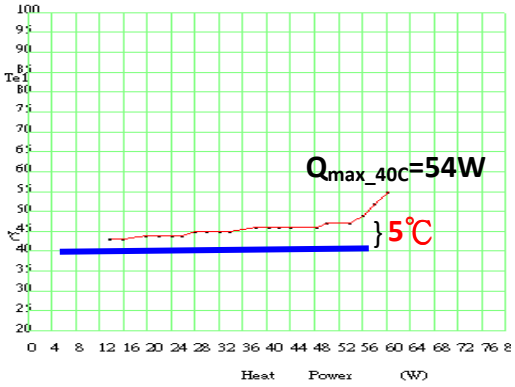

Fig. 4. The heat pipe performance curve

Table 1. Heat pipe geometry parameters

$2R_{HP,O}$ (mm)	$2R_{HP,i}$ (mm)	$2R_i$ (mm)	L_{tot} (mm)	r_w (mm)
6	5	4	185	0.078
$K_w \times 10^{10}$ (m^2)	$A_w \times 10^6$ (m^2)	Wick type	δ_{wall} (mm)	$V_{pore} \times 10^7$ (m^3)
1.225	4.775	sinter	0.9	7.166
ε	$V_{tot} \times 10^6$ (m^3)	β		
0.548	3.041	23.6		

Table 2. Comparison the Q_{max_40C} of the theoretical value and the experimental data at 40℃ and different inventory.

Working fluid	P_{NCG} (torr)	$Q_{max\_40C\_theory}$ (W)	$Q_{max\_40C\_exp}$ (W)	Er.1 (%)
0.7ml	0.1	4	4	0
	0.5	3.88	4	3
	1	3.74	4	6.9
	5	2.77	3	8.3
	10	1.91	2	4.7
0.8ml	0.1	8	8	0
	0.5	7.76	7.99	2.9
	1	7.48	7.97	6.4
	5	5.55	5.99	7.4
	10	3.82	4	4.6
0.9ml	0.1	6	6	0
	0.5	5.82	5.97	2.6
	1	5.61	5.97	6.4
	5	4.16	4	3.8
	10	2.86	2.99	4.5
1ml	0.1	5.01	5.01	0
	0.5	4.86	5	2.8
	1	4.69	4.99	6.4
	5	3.48	3.8	9.2
	10	2.39	2.2	7.9
1.1ml	0.1	4	4	0
	0.5	3.88	4	3
	1	3.74	4	6.9
	5	2.77	3	8.3
	10	1.91	2	4.7

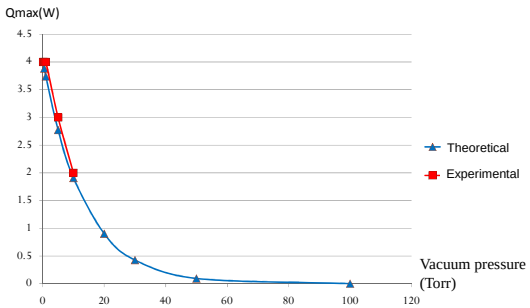

Fig. 5. Q_{max_40C} With respect to vacuum pressure for theoretical value and experimental data,at inventory 0.7ml

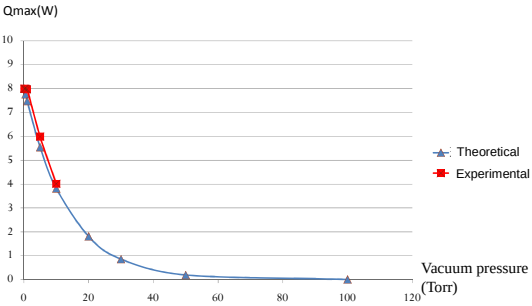

Fig. 6. Q_{max_40C} With respect to vacuum pressure for theoretical value and experimental data,at inventory 0.8ml

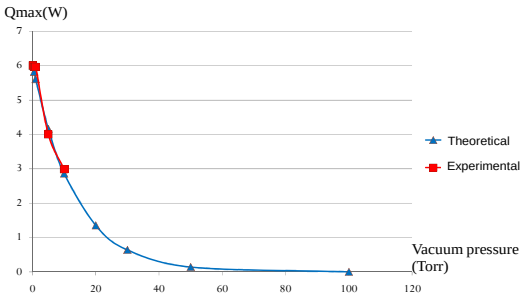

Fig. 7. Q_{max_40C} With respect to vacuum pressure for theoretical value and experimental data,at inventory 0.9ml

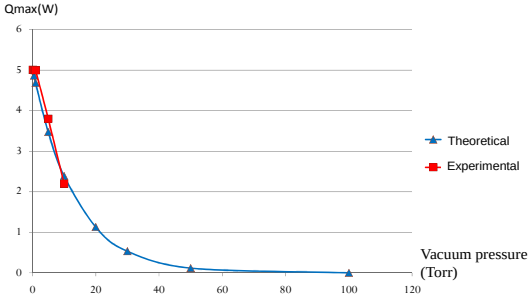

Fig.8. Q_{max_40C} With respect to vacuum pressure for theoretical value and experimental data,at inventory 1.0ml

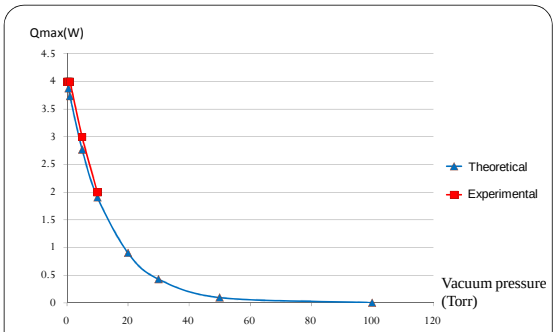

Fig. 9. Q_{max_40C} With respect to vacuum pressure for theoretical value and experimental data,at inventory 1.1ml

Table 3. Comparison of the Q_{max_40C} at different inventory for P_{NCG} =0 and T_a=40℃.

working fluid inventory: 0.7ml				
P_{NCG} (torr)	$Q_{max\_40C\_exp}$ (W)	$Q_{max\_40C,0}$ (W),P_{NCG}=0	$Q_{max\_40C,0,avg}$ (W)	Er.2 %
0.1	4	4.03	4.21	4.3
0.5	4	4.15		1.4
1	4	4.31		2.4
5	3	4.36		3.6
10	2	4.22		0.2
working fluid inventory: 0.8ml				
P_{NCG} (torr)	$Q_{max\_40C\_exp}$ (W)	$Q_{max\_40C,0}$ (W),P_{NCG}=0	$Q_{max\_40C,0,avg}$ (W)	Er.2 %
0.1	8.01	8.06	8.42	4.3
0.5	7.99	8.29		1.5
1	7.97	8.59		2.0
5	5.99	8.7		3.3
10	4	8.45		0.3
working fluid inventory: 0.9ml				
P_{NCG} (torr)	$Q_{max\_40C\_exp}$ (W)	$Q_{max\_40C,0}$ (W),P_{NCG}=0	$Q_{max\_40C,0,avg}$ (W)	Er.2 %
0.1	6.01	6.05	6.16	1.8
0.5	5.97	6.2		0.6
1	5.97	6.43		4.4
5	4	5.81		5.7
10	2.99	6.31		2.4

working fluid inventory: 1ml				
P_{NCG} (torr)	$Q_{max\_40C\_exp}$ (W)	$Q_{max\_40C,0}$ (W),P_{NCG}=0	$Q_{max\_40C,0,avg}$ (W)	Er.2 %
0.1	5.01	5.05	5.16	2.1
0.5	5	5.19		0.6
1	4.99	5.38		4.3
5	3.8	5.52		7.0
10	2.2	4.7		8.9
working fluid inventory: 1.1ml				
P_{NCG} (torr)	$Q_{max\_40C\_exp}$ (W)	$Q_{max\_40C,0}$ (W) ,P_{NCG}=0	$Q_{max\_40C,0,avg}$ (W)	Er.2 %
0.1	4	4.03	4.21	4.3
0.5	4	4.15		1.4
1	4	4.31		2.4
5	3	4.36		3.6
10	2	4.22		0.2

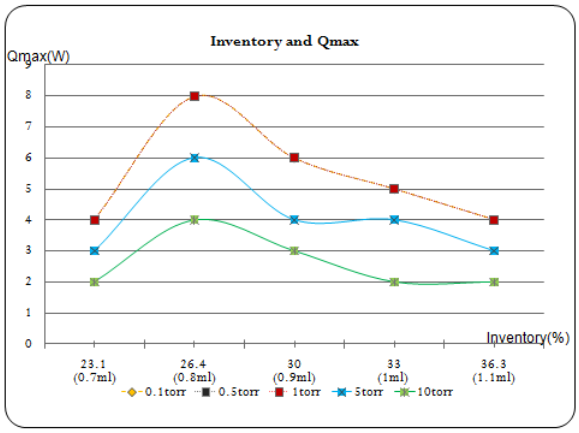

Fig. 10. Effect of the inventory to the maximum heat loading of the heat pipe

Table 4. The indicator for working fluid inventory in heat pipe

Inventory (ml)	V^+	β	1>V+>β
0.7	0.231	0.236	unsatisfied
0.8	0.264		satisfied
0.9	0.297		satisfied
1	0.3		satisfied
1.1	0.363		satisfied

5. CONCLUSIONS

The maximum heat loading with respect to different working inventory had been successfully developed in this study, experiment results was also match with the theoretical data. The following were the summary:

a. The lower the non-condensable gas, the higher the maximum heat loading of the heat pipe.
b. The working fluid inventory must larger than the pore volume in the wick.
c. There exist a optimal inventory quantity, the proposed volume was 1.118 times the pore volume in the wick for this study.
d. the impact for the working fluid inventory less than Vpore was greater than that of the volume larger than the Vpore.

6. NOMENCLATURE

symbol	description
A_w	wick cross sectional area, m^2
A_i	cross sectional area for vapor channel, m^2
f'	friction factor for liquid and vapor at axial direction
g	Acceleration of gravity, m/s^2
h_{fg_Ta}	latent heat at the operating temperature T_a, kJ/kg
K_w	Permeability, m^2
L_a	adiabatic length of heat pipe, m
L_c	condenser length of the heat pipe, m
L_e	evaporator length of the heat pipe, m
L_{eff}	effect length of heat pipe, m
M_f	total friction factor due to viscosity and wick effect from liquid and vapor
m_l	working fluid inventory, ml
P_{NCG}	pressure of non-condensable gas, kPa
Q_{max_Ta}	Maxmun heat loading of the heat pipe at the operating temperature (T_a), W
$Q_{max\_Ta,0}$	Maxmun heat loading of the heat pipe without any non-condensable gas and at the operating temperature (T_a), W
r_w	wick radius, m
R_i	radius for vapor channel (wick inner radius), m
R_0	wick out radius, m.
V_{pore}	the space volume of the wick, m^3
V_{tot}	total space volume of the heat pipe, m^3
V^+	ratio of the inventory to the product of the V_{tot} andρ_l
ψ	tilt for heat pipe
μ_l	liquid viscosity, $N\cdot s/m^2$
ΔP_c	capillary pressure drop， kPa
ΔP_{cg}	pressure difference between capillary and gravitation
ΔP_l	pressure drop due to liquid flow, kPa
ΔP_v	pressure drop due to vapor flow, kPa

ΔP_g	gravitational pressure drop, kPa
ρ_l	liquid density, kg/m^3
ρ_v	vapor density, kg/m^3
σ_l	liquid surface tension, N/m
ε	porosity of the wick structure
β	ratio of the space volume of the wick to the total space volume of the heat pipe

ACKNOWLEDGEMENT

This study is the National Science Council's NSC-100-3113-E-006-002 project. We are grateful for the NSC's support, which has allowed the successful implementation of this project.

7. REFERENCES

[1] A. Faghri, Heat Pipe Science and Technology Taylor & Francis, 1995.

[2] Sauciuc, The Design and Testing of the Super Fiber Heat pipes for Electronics Cooling, IEEE, Sixteenth IEEE SEMI-THERM (2000) 27–32.

[3] F. Kreith, M.S. Boh, Principles of Heat Transfer, Books/Cole, 2001 .

[4] S.H. Moon, Experimental Study on the Performance of Miniature Heat Pipes with Woven-Wire Wick, IEEE Transaction on Components and Packing Technologies 24 (4) (December, 2001) 1521–3331.

[5] H.W. Lin, Yi.X. Zheng, Wei.K. Lin, T.B. Chang, An Axial Heat Conduction Model to Predict the Maximum Heat Removed of the Miniature Heat Pipe, *Transactions of the Aeronautical and Astronautical Society of the Republic of China* 35 (4) (2003) 393–400.

[6] Chun-Chang Lu, Wei-Keng Lin, "The vacuum measurement theory of Heat Pipe", Journal of Advanced Engineering (JAE) (EI) , Vol. 4, No. 4, pp.331-335, Oct. 2009.

[7] Dunn, P. &, Reay, D. A., "Heat Pipes." Pergamon Press, 1976